

1 **Inundation of Stormwater Infrastructure is Common and Increases Risk of Flooding**  
2 **in Coastal Urban Areas**

3  
4 **Adam C. Gold<sup>1</sup>, Chelsea M. Brown<sup>2</sup>, Suzanne P. Thompson<sup>2</sup>, and Michael F. Piehler<sup>1,2</sup>**

5  
6 <sup>1</sup> Institute for the Environment, University of North Carolina at Chapel Hill, 100 Europa Dr.  
7 Suite 490, Chapel Hill, NC 27517, USA.

8  
9 <sup>2</sup> Institute of Marine Sciences, University of North Carolina at Chapel Hill, 3431 Arendell Street,  
10 Morehead City, NC 28557, USA.

11  
12 Corresponding author: Adam Gold ([gold@unc.edu](mailto:gold@unc.edu))

13  
14 **Key Points:**

- 15
- 16 • Proxy measurements show that inundation of coastal stormwater networks from high  
17 receiving water levels is common along the US east coast
  - 18 • Water level measurements and modeling in coastal North Carolina showed frequent  
19 stormwater network inundation at typical water levels
  - 20 • Stormwater network inundation increases risk of overland flooding in coastal urban areas

## 21 **Abstract**

22 Stormwater infrastructure can mitigate precipitation-driven flooding when there are no  
23 obstructions to draining. Coastal areas increasingly experience recurrent flooding due to elevated  
24 water levels from storms or tides, but the inundation of coastal stormwater infrastructure by  
25 elevated water levels has not been broadly assessed. We conservatively estimated stormwater  
26 infrastructure inundation in municipalities along the Atlantic United States coast by using areas  
27 of high tide flooding (HTF) on roads as a proxy. We also modeled stormwater infrastructure  
28 inundation in four North Carolina municipalities and measured infrastructure inundation in one.  
29 Over 600 east coast municipalities had road area impacted by HTF, and over 1/3<sup>rd</sup> had >1% road  
30 area impacted. Modeling results and water level measurements indicated that extensive  
31 inundation of underground stormwater infrastructure frequently occurs during typical water  
32 levels. These results suggest that stormwater infrastructure inundation is common and increases  
33 the occurrence of urban flooding along the east coast of the US.

34

## 35 **1 Introduction**

36 Coastal flooding is a longstanding issue which has been exacerbated by climate change  
37 (Kulp & Strauss, 2019; Nicholls et al., 1999; Wahl et al., 2015; Woodruff et al., 2013). Flooding  
38 due to extreme storm events such as hurricanes is increasing, and these extreme storms can cause  
39 massive amounts of damage to coastal communities (Hallegatte et al., 2013; Hinkel et al., 2014).  
40 While sea level rise is predicted to increase the impact of extreme storm events on coastal areas,  
41 it is also increasing the incidence of recurrent nuisance flooding known as “high tide flooding”  
42 (HTF) (Sweet et al., 2020, 2018). Many cities in the United States (US) already experience  
43 multiple days of HTF a year, with the number of flood days rapidly increasing (Sweet et al.,

44 2018). During dry weather, this recurrent nuisance flooding can be disruptive to local  
45 infrastructure and economies (Hino et al., 2019; Jacobs et al., 2018). Combined with typical  
46 storm conditions, high tide flooding can impede stormwater drainage and result in more  
47 significant compound flooding (Rosenzweig et al., 2018; Shen et al., 2019; Wahl et al., 2015;  
48 R.L. Wilby, 2007).

49 Stormwater drainage networks aim to prevent flooding from stormwater runoff, but sea  
50 level rise threatens to reduce the efficacy of coastal stormwater networks (Rosenzweig et al.,  
51 2018; Titus et al., 1987; R.L. Wilby, 2007). The goal of reducing precipitation-driven flooding  
52 has conventionally been achieved using an underground pipe network that quickly conveys  
53 stormwater runoff to a receiving waterbody using gravity (Burns et al., 2012; Hale, 2016). Older  
54 stormwater networks were designed to accommodate conditions at the time of their construction  
55 under the assumption that future conditions and variability will be similar to those in the past, but  
56 climate change has invalidated this assumption (Milly et al., 2008). Relative sea level rise in  
57 some coastal areas of the US has increased mean sea level by up to a foot since the 1960s  
58 (Eggleston & Pope, 2013; Zervas, 2009), so many coastal stormwater networks are increasingly  
59 inundated by typical high tide water levels or rising groundwater levels (Rotzoll & Fletcher,  
60 2013; Sadler et al., 2020; Shen et al., 2019; Su et al., 2020; Wdowinski et al., 2016). Stormwater  
61 network inundation reduces how well the system drains during storm events (Shen et al., 2019;  
62 Wahl et al., 2015), but recurrent stormwater network inundation by saltwater also corrodes  
63 stormwater infrastructure (Bjerklie et al., 2012), promotes saltwater intrusion to groundwater (Su  
64 et al., 2020), and can mobilize fecal bacteria from co-located sanitary sewer lines (Su et al.,  
65 2020).

66           Inundation of underground stormwater networks has been reported in multiple cities in  
67 the US (Hino et al., 2019; Sadler et al., 2020; Shen et al., 2019; Wdowinski et al., 2016), but a  
68 broad characterization of stormwater network inundation has not been conducted. Recent studies  
69 of compound flooding show how both stormwater network inundation and precipitation  
70 influence coastal flooding, but most of these studies focus on small areas or specific extreme  
71 storm events to recreate real-world flooding conditions using hydrodynamic models (Gallien et  
72 al., 2014; Hasan Tanim & Goharian, 2020; Sadler et al., 2020; Shen et al., 2019). These flooding  
73 estimates are extremely useful for the modeled study areas, but the limited spatial or temporal  
74 resolution of flooding estimates may limit their utility to identify vulnerable infrastructure  
75 hotspots at larger spatial scales or during dry-weather conditions. Regional- or national-scale  
76 estimates of stormwater network inundation do not exist, but these estimates, or even proxies, of  
77 stormwater network inundation would be helpful in characterizing the extent and scale of the  
78 issue. For broad estimates of stormwater network inundation to identify vulnerable infrastructure  
79 during dry- or wet-weather conditions, static inundation (“bathtub”) models that use a digital  
80 elevation model (DEM) to estimate inundation at discrete water levels may serve as useful tools  
81 for managers. Static inundation models have limitations, such as over-estimating flooding extent  
82 relative to hydrodynamic models (Castrucci & Tahvildari, 2018; Gallien et al., 2014), but their  
83 simplicity makes them well-suited for use as a diagnostic tool at large spatial scales.

84           In this study, we used simple proxies, static inundation models, and water level  
85 measurements to estimate stormwater network inundation at varying spatial scales. Through  
86 modeling, we also tested how stormwater networks influence flooding when receiving waters are  
87 elevated and how stormwater network inundation relates to current NOAA coastal flood  
88 thresholds. To identify locations along the eastern US coast where stormwater network

89 inundation may occur, we used buffered road data from the OpenStreetMap and NOAA high tide  
90 flooding estimates to find roads within incorporated municipalities that experience HTF, and  
91 thus likely also have subterranean inundation of the stormwater network draining the road. To  
92 characterize inundation of the stormwater network in the coastal town of Beaufort, NC, we  
93 measured water levels in stormwater infrastructure over a period of 8 months and compared them  
94 to water levels from a nearby NOAA tide gauge (Figure S1). We then used a static inundation  
95 model both with and without a coupled pipe network model to estimate stormwater network  
96 inundation and overland flooding across a range of water levels in Beaufort and three other cities  
97 in NC (Wilmington, Nags Head, and New Bern)(Figure S1).

98

## 99 **2 Materials and Methods**

### 100 2.1 High tide flooding on roads along the US east coast

101 We used publicly available national-scale road and high tide flooding datasets to find  
102 areas where the two datasets overlapped in incorporated municipalities along the east coast of the  
103 US. We suggest that areas where roads are inundated during high tide flooding can act as a  
104 conservative proxy for areas where stormwater network inundation occurs during high tide  
105 events. This estimate can be considered conservative because without stormwater network  
106 infrastructure data, we cannot estimate the extent of inundation in pipes that are underground.  
107 Therefore, the only way to estimate the incidence of underground stormwater network  
108 inundation at a national or regional scale is to detect the end results of stormwater network  
109 inundation, which is overland flooding caused by surcharge from the stormwater network or  
110 overland flooding that is actively entering the stormwater network. This assumption would likely

111 not apply in lower-density or rural areas if there is no stormwater network present, but we  
112 believe that this assumption is reasonable within the boundaries of incorporated municipalities.

113         The east coast of the US is comprised of fifteen states, ranging from the Atlantic coast of  
114 Florida to Maine, and these fifteen states were selected as the extent for the stormwater network  
115 inundation estimate. Census bureau incorporated municipality boundaries were downloaded for  
116 each state in order to constrain the estimate to urban areas, where the underlying assumption of  
117 the coincidence of roads and stormwater networks is likely strongest. High tide flooding  
118 estimates from NOAA were downloaded for each state (Sweet et al., 2020), and these estimates  
119 consist of approximately 3-meter resolution raster data sets that indicate areas where “minor  
120 flooding” occurs based on a common impact threshold derived from the local tidal range (Minor  
121 flood threshold (m) =  $1.04 * (\text{Mean Higher High Water} - \text{Mean Lower Low Water}) + 0.5$ )  
122 (Sweet et al., 2018). Road data for each state were downloaded from the open-source  
123 OpenStreetMap (<https://www.openstreetmap.org>). The OpenStreetMap road dataset was selected  
124 rather than the Census Bureau’s TIGER dataset because the OpenStreetMap dataset explicitly  
125 identifies bridges and tunnels. Bridges and tunnels were removed from the roads dataset because  
126 including bridges and tunnels could create false positives for the inundation estimates, where the  
127 bridge or tunnel appears to overlap high tide flooding extent when it is actually over (bridges) or  
128 under (tunnels) the inundated area; most bridges are removed from the DEMs used to calculate  
129 high tide flooding estimates.

130         Processed road data consisted of GIS polylines, and a 5-meter buffer was created around  
131 all polylines to create polygons that approximated road surfaces (i.e., 10 meter width).  
132 Waterbody outlines from the National Hydrography Dataset (NHD) (i.e., ocean/sea, rivers,  
133 ponds, reservoirs) were used to remove any portions of buffered roads that intersected them to

134 further remove false positive areas. Polygons representing buffered roads were then used to  
135 extract high tide flooding estimates. The extracted high tide flooding estimates were then used to  
136 clip the buffered road network, so that the attributes associated with the buffered road polygons  
137 could be analyzed (i.e., road type). Areas of overlap among buffered roads where road area  
138 would be counted multiple times were extracted and dissolved to create polygons labeled simply  
139 “intersection”. These intersection areas were erased from the buffered road polygon dataset to  
140 remove the overlapping polygon areas, and then the intersection areas were merged with the  
141 edited buffered road polygon dataset.

142 This analysis resulted in areas where high tide flooding estimates intersect roads,  
143 assuming a 10m wide road. Based on the assumptions outlined above, these data represented  
144 areas where stormwater network inundation may occur, either from surcharge from the  
145 stormwater network due to tidal flooding or from tidal flooding overtopping stormwater network  
146 inlets.

147

## 148 2.2 Site Description

149 We measured various stormwater network water levels and modeled inundation in  
150 Beaufort, a small town located in coastal North Carolina on a peninsula between the mouths of  
151 the Newport and North Rivers (Figure S1). The downtown area of Beaufort is located directly  
152 adjacent to Taylor’s Creek, a channel that receives either brackish flow from the Newport/North  
153 rivers or saline water from the Atlantic Ocean via Beaufort Inlet. Taylor’s Creek has a mean  
154 semi-diurnal tidal range of 3.11 ft (NOAA gage 8656483). The downtown area has moderate  
155 urban land use and uses conventional subsurface piping to convey stormwater from impervious  
156 surfaces directly to Taylor’s Creek. The town has no stormwater backflow measures, and often

157 documents “sunny day” high-tide flooding and compound flooding during storm events (Sweet  
158 et al., 2020). A recent survey of the stormwater network by a civil engineering firm produced  
159 measurements for most of the downtown area (shown in bold in Figure S1).

160 Stormwater network inundation was also modeled in Wilmington, New Bern, and Nags  
161 Head, North Carolina. Each dataset had sporadic missing values for pipe or structure elevations,  
162 but New Bern had a large section of upland new development that was excluded due to missing  
163 survey elevations. All three cities (and Beaufort) have some distinctly different characteristics,  
164 but they all have all have flooding issues and large areas of development that rely on subsurface  
165 stormwater conveyance directly to a receiving waterbody. Wilmington is both the largest city  
166 and the city with highest elevation and relief. Wilmington’s downtown area is directly adjacent  
167 to the Cape Fear River and has a mean semi-diurnal tidal range of 4.28 ft above the river stage  
168 (NOAA gage 8658120), but it also has extensive suburban land use on the southern and eastern  
169 sides of the city that are affected by mean 3.98 ft semi-diurnal tides from the Atlantic Ocean  
170 (NOAA gage 8658163). New Bern is further inland and lies on the western side of the Neuse  
171 River. The Neuse River near New Bern can experience large amounts of riverine or storm surge  
172 flooding during hurricanes due to its eastward-facing orientation, and this occurred recently in  
173 2018 during Hurricane Florence that led to damages costing hundreds of millions of dollars.  
174 Nags Head is located on the Outer Banks, east of Manteo and Roanoke Island. On its western  
175 side, Nags Head is affected by wind-driven tides within the Pamlico sound, while its eastern side  
176 is affected by mean 3.22 ft semi-diurnal tides (nearby NOAA gage 8651370) from the Atlantic  
177 Ocean.

178



### 179 2.3 Water level

180 Two stormwater outfalls in Beaufort were selected for water level monitoring (Figure S1,  
181 OS-outfall and MP-outfall), and water level within the pipes was measured every 30 minutes  
182 from June 2017 to February 2018 (8 months) using a Teledyne Isco low-velocity flow sensor  
183 (pressure transducer for level) . In late November (for 3 months), we began measuring water  
184 level in a storm drain upstream from the MP site (Figure S1, MP-upstream).

185 A NOAA water level gauge located in Beaufort on Taylor's Creek, and data were  
186 downloaded from this station to compare to our measured water levels. Using NOAA water level  
187 data and the surveyed invert elevations of our monitored sites (NAVD88), the water level in each  
188 monitored site was estimated every 30 minutes, coincident with the measured water levels within  
189 the pipes. Pipe diameter measurements for the two monitored outfalls and one storm drain were  
190 used to calculate the percent cross-sectional area inundated at the pipe ends for each time step of  
191 measured water level.

192

### 193 2.4 Inundation Modeling

194 Stormwater network GIS data were obtained from each individual municipality by  
195 request. In total, we contacted 14 municipalities in coastal North Carolina and received data from  
196 8 municipalities. After data QC, we determined that only 5 municipalities had adequate data for  
197 the purpose of inundation modeling, and the main selection criteria were data coverage of the  
198 majority of the city and elevation or depth data for stormwater inverts. We chose four  
199 municipalities with good quality data: Beaufort, Wilmington, Nags Head, and New Bern.

200 We then created an R package, *bathtub* (<https://acgold.github.io/bathtub/>), that  
201 implements a 2D static inundation model coupled with a 1D pipe network model to estimate

202 stormwater network inundation at discrete water levels. The R package uses GIS data  
203 representing the stormwater network features (e.g., pipes, drop inlets, junction boxes, etc.), and  
204 creates a model object consisting of 3 simple feature objects (*sf* R package, Pebesma, 2018):  
205 ‘pipes’, ‘nodes’ (pipe ends), and ‘structures’ (e.g., drop inlet, junction box, etc.). Network  
206 connectivity derived from the spatial topology is stored in the ‘nodes’ layer. In the case of the  
207 occasional missing invert elevation at a node, the value is conservatively interpolated from  
208 nearby nodes by dropping the invert elevation a minimal amount (0.1 feet) from the nearest up-  
209 network value.

210 For the 2D inundation model, we used methods and source data used by NOAA to model  
211 overland inundation (SLR viewer: <https://coast.noaa.gov/slr/>). We utilized 1/9<sup>th</sup> arcsecond (~ 3  
212 m) NOAA SLR DEMs (<https://coast.noaa.gov/slrdata/>) and converted the vertical datum of the  
213 elevation values from NAVD88 to the local mean higher high water (MHHW) datum using a  
214 conversion raster created with the NOAA VDATUM application  
215 (<https://coast.noaa.gov/htdata/Inundation/TidalSurfaces>). For Nags Head only, the conversion  
216 factor between NAVD88 and MHHW was propagated up the stormwater network because there  
217 were large differences in conversion factors between the western side (Pamlico Sound) and  
218 eastern side (Atlantic Ocean) of the barrier island. For each distinct water level modeled, areas  
219 lower than that elevation were selected, and clumps of cells smaller than a specified area were  
220 removed. This filtering of small clumps of cells ensured that modeled inundation only  
221 represented areas connected to the receiving water body.

222 This estimate of overland flooding was used as a starting point for the 1D pipe model,  
223 with all nodes (pipe ends) that intersected the overland flooding extent selected and marked as  
224 “impacted” at that water level. The specified water level was propagated up-network by

225 evaluating every node connected to the initially-selected nodes by a pipe and selecting nodes  
226 with invert elevations below the specified water level. This propagation continued until no  
227 additional nodes were selected for the specified water level. All selected nodes and both pipes  
228 and structures connected to them were marked as “impacted”, and using the diameter of each  
229 pipe end and the depth of each structure, the percent inundation of each object was calculated.  
230 Overland ponding was estimated using the original MHHW DEM by selecting all cells under the  
231 specified elevation and selecting only clumps of cells not connected to downstream waters but  
232 intersected structures that were estimated to be surcharging (water elevation > surface structure  
233 elevation).

234 Error estimates for model results were calculated using the z-score mapping method  
235 (Schmid et al., 2014), which produces a p-value that indicates the likelihood of inundation at a  
236 particular water level for each DEM pixel or stormwater network component. For the 2D model,  
237 error estimates incorporated the root mean squared error (RMSE) of the source DEM and the  
238 error associated with converting elevations from NAVD88 to MHHW. For this study, RMSE of  
239 the source NOAA DEM was 20 cm while estimated error (as standard deviation) of the  
240 conversion factor was 10 cm. In computing z-scores for stormwater network components, the  
241 measurement error of network invert elevations (estimated at 10 cm) was added to the error  
242 components from the 2D model if invert elevations were derived from depth measurements. If  
243 invert elevations were directly measured, the only additional error included was error from the  
244 conversion between NAVD88 and MHHW. P-values derived from z-scores allowed for  
245 predicted impacted infrastructure to be classified as “high confidence” (80% confidence,  $p < 0.2$ )  
246 or “low confidence” (20% confidence,  $p < 0.8$ ).

247 Using the *bathtub* R package, we modeled inundation in all four study cities between the  
248 water levels of -3 ft and 4 ft MHHW by 0.25 ft increments. To estimate flooding caused by  
249 stormwater network surcharge, the number of inlet structures impacted at each water level  
250 estimated by the 2D-1D model were compared to the number of inlet structures impacted by only  
251 the 2D component of the model that represents overland flooding with no subsurface modeling.

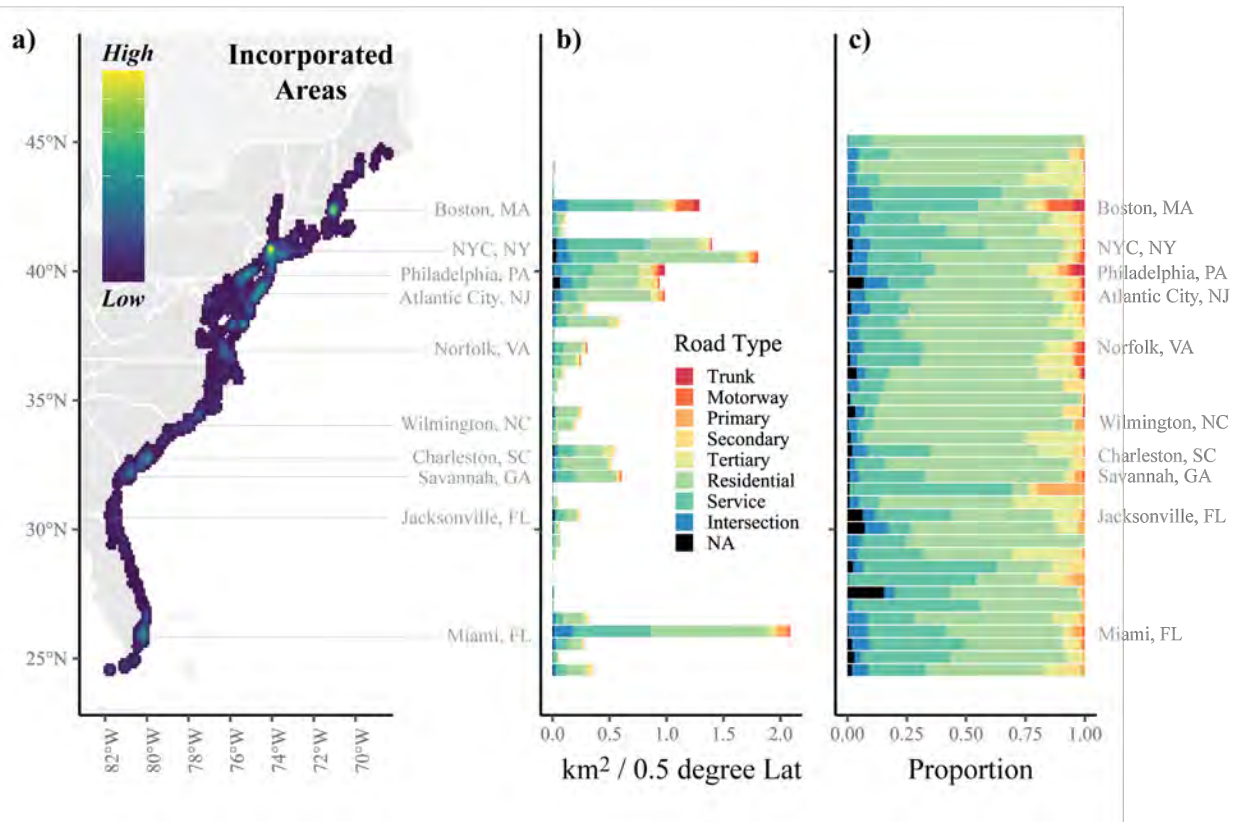
252

### 253 **3 Results**

#### 254 3.1. High tide flooding on roads along the US east coast

255 High tide flooding on roads was estimated to occur to some extent in 656 incorporated  
256 municipalities along the US east coast, indicating that inundation of stormwater infrastructure  
257 may occur in many of these municipalities during high tide unless backflow measures exist  
258 (Figure 1). The metro areas of Miami, FL, New York City, NY, and Boston, MA had the largest  
259 estimated extent of high tide flooding on roads, partially because of the overall large amount of  
260 roads (Figure 1a,b, Figure 2). The majority of estimated impacted roads are classified as service  
261 (e.g., parking lots, alleys, etc.) or residential roads, but larger and higher-traffic roads (tertiary –  
262 trunk) were also estimated to be impacted in larger metro areas (Figure 1b,c).

263



264

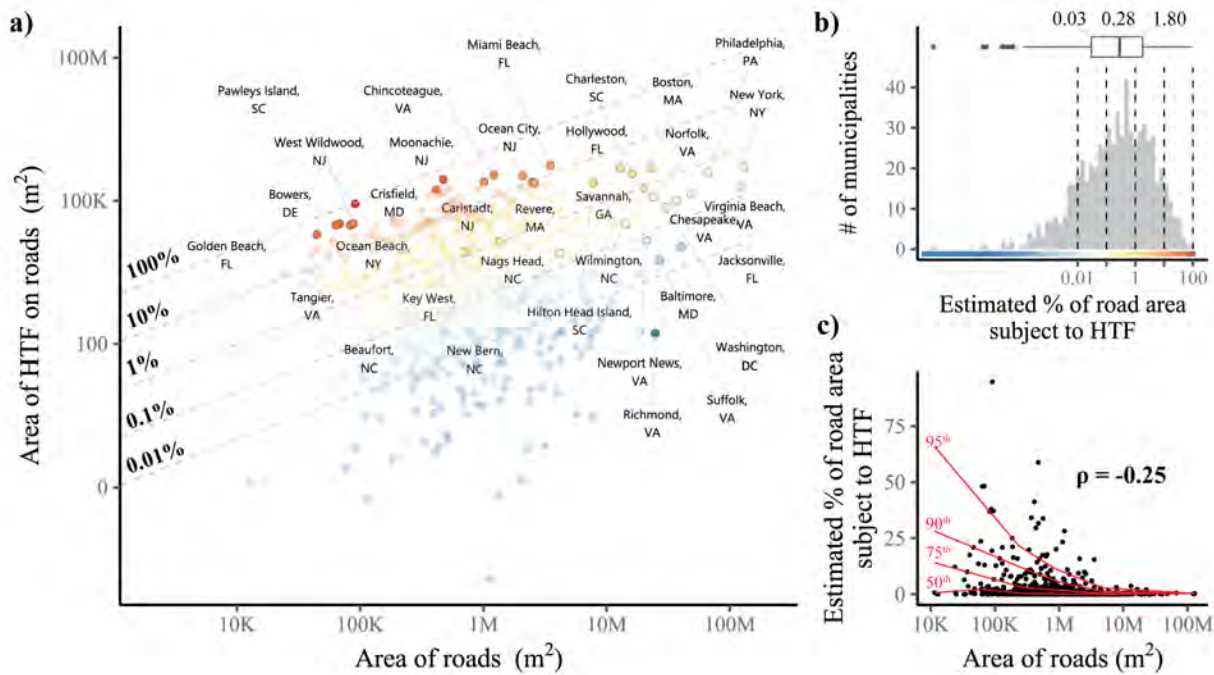
265 **Figure 1.** Area of high tide flooding on city roads. **a)** Density map of areas where high tide  
 266 flooding overlaps roads in incorporated areas, **b)** road area overlapping estimated high tide  
 267 flooding extent binned by 0.5 degrees of latitude, and **c)** proportion of impacted road area  
 268 separated by road type.

269

270 Using estimates of total road area for each incorporated municipality, we found that the  
 271 median percent of total road area impacted by HTF decreased as total road area increased ( $\rho = -$   
 272  $0.25$ ,  $p < 0.001$ , Figure 2), and the relative impact of HTF on roads varied greatly between  
 273 municipalities, ranging from just over 0 to 94.5% of total road area impacted by HTF. While a  
 274 majority of municipalities along the US east coast that currently experience HTF on roads had  
 275 relatively small amounts of total road area impacted by HTF (median = 0.28%, Figure 2),  
 276 approximately 1/3<sup>rd</sup> of the municipalities had greater than 1% of total road area impacted by HTF  
 277 and approximately 13% of the municipalities had greater than 5% of total road area impacted  
 278 HTF (Figure 2). Of the four municipalities measured or modeled in this study, Beaufort had the

279 highest percent of total road area impacted by HTF (1.17%), followed by Nags Head (1.04%),  
 280 Wilmington (0.23%), and New Bern (0.19%).

281



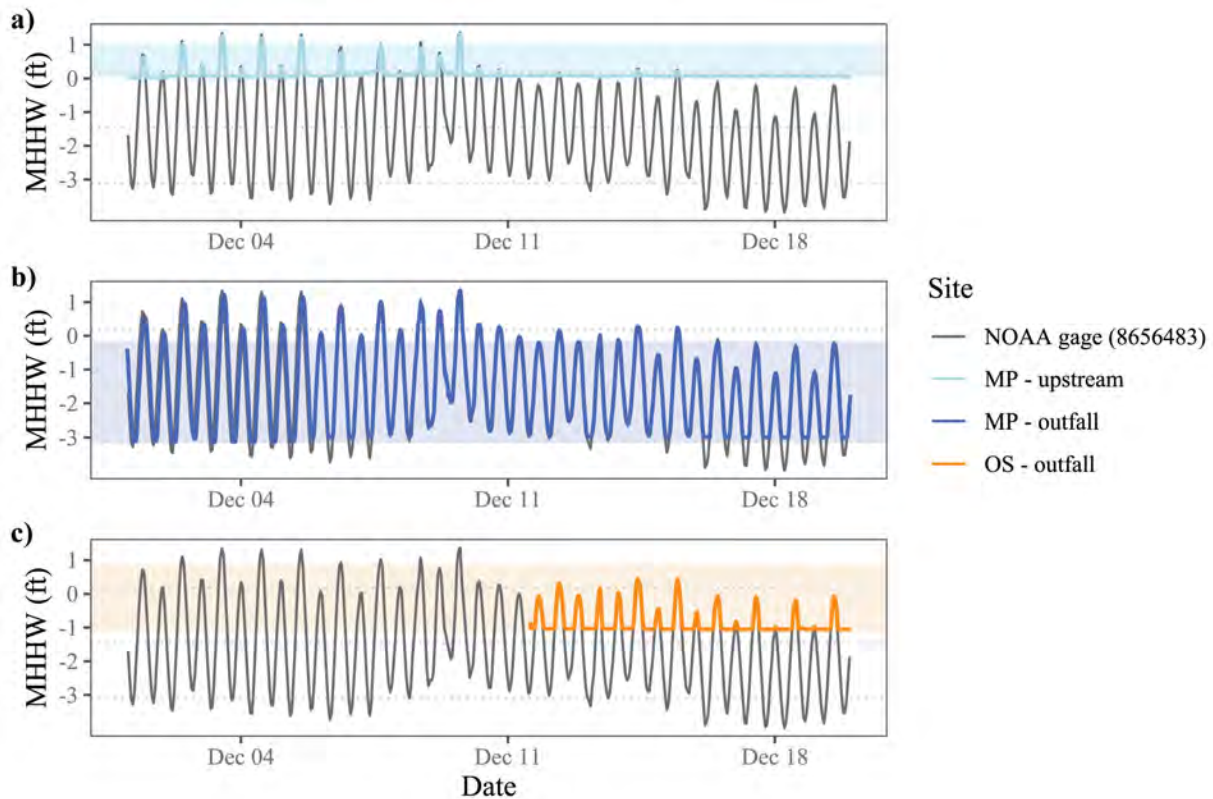
282

283 **Figure 2.** High tide flooding on city roads compared to total road area. **a)** Road area affected by  
 284 high tide flooding (HTF) versus total road area for municipalities along the US east coast that  
 285 experience some degree of HTF. Dotted lines and color indicate the estimated percent of road  
 286 area subject to HTF in each municipality. Selected municipalities labeled, including the four  
 287 study municipalities. **b)** Histogram of percent of total road area impacted by HTF. **c)** Percent of  
 288 total road area impacted versus total road area with smooth quantiles (red).  
 289

### 290 3.2 Measured water levels

291 In Beaufort, NC, the two monitored stormwater outfalls experienced some degree of tidal  
 292 inundation every tidal cycle throughout the 8-month monitoring period. (data shown for  
 293 December 2017 in Figure 3). The upstream monitored storm drain (MP-upstream) was located  
 294 more than 200 meters up-network from the corresponding outfall (MP-outfall), but MP-upstream  
 295 also experienced significant tidal inundation during more extreme high-tide events (Figure 3).  
 296 Water level in each monitored outfall was predicted based on NOAA water level from a nearby

297 gauge and the invert elevation of the infrastructure. Predicted water level measurements  
 298 corresponded well with observed water levels ( $r^2 = 0.72 - 0.95$ ), as did cumulative distribution  
 299 functions of predicted and observed pipe inundation percent (Figure S2). The predicted water  
 300 levels for the MP-upstream site were slightly higher than the measured water levels, and the  
 301 predicted cumulative distribution of inundation percent over-predicted the occurrence of small  
 302 amounts of inundation in the storm drain (Figure S2).  
 303



304

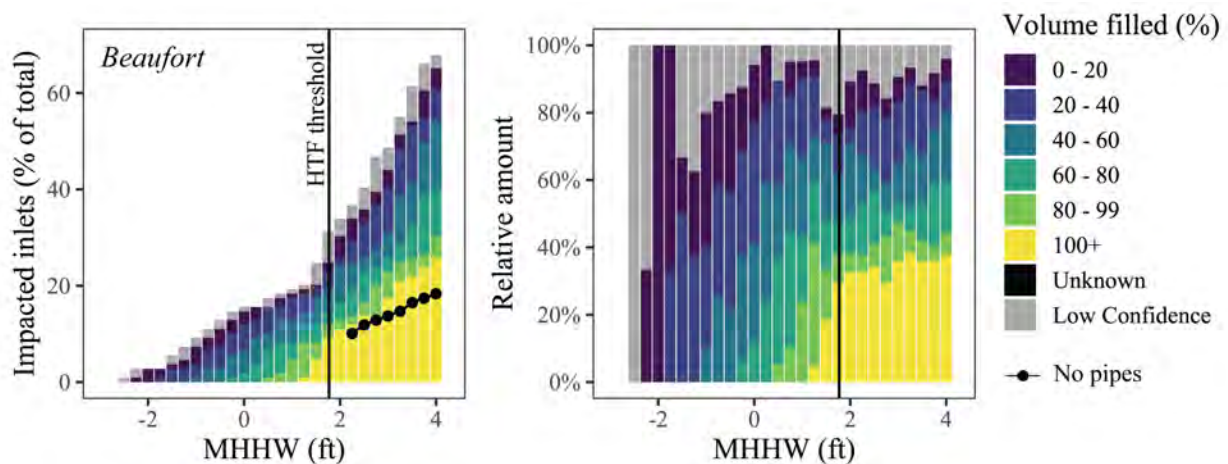
305 **Figure 3.** Snapshot of measured water levels in pipes. Example of water level measured in  
 306 selected pipes (color lines) and a NOAA tide gage in Beaufort, NC (grey line) in December  
 307 2017. Shaded areas represent the dimensions of the pipe, showing that the monitored pipes were  
 308 frequently filled with water from the receiving water body. Water level from OS – outfall (panel  
 309 a) is missing on the graph prior to Dec 11 due to equipment malfunction.  
 310



## 311 3.3. Inundation modeling

312 Modeling the impacts of a range of water levels on stormwater infrastructure inundation  
 313 for the Town of Beaufort showed that the stormwater network likely has extensive inundation at  
 314 typical water levels (mean sea level = -1.83 MHHW, mean high water = -0.29 ft MHHW)(Figure  
 315 4). At lower water levels, the inundation estimates are completely subsurface (Figure 4, Figure  
 316 5a), but beginning around 1.5 – 2 ft MHHW (near NOAA HTF threshold), portions of the  
 317 stormwater network reach full capacity and result in surcharging and ponding on roadways  
 318 (Figure 4, Figure 5c). Model simulations that do not incorporate conveyance via the stormwater  
 319 network show overland flooding due to shoreline overtopping at 2.25 ft MHHW (Figure 5b), and  
 320 the estimated number of stormwater inlets impacted by solely overland flooding (“no pipes” line  
 321 in Figure 4) is consistently smaller than the estimated number of inlets that are at full capacity  
 322 (Figure 4).

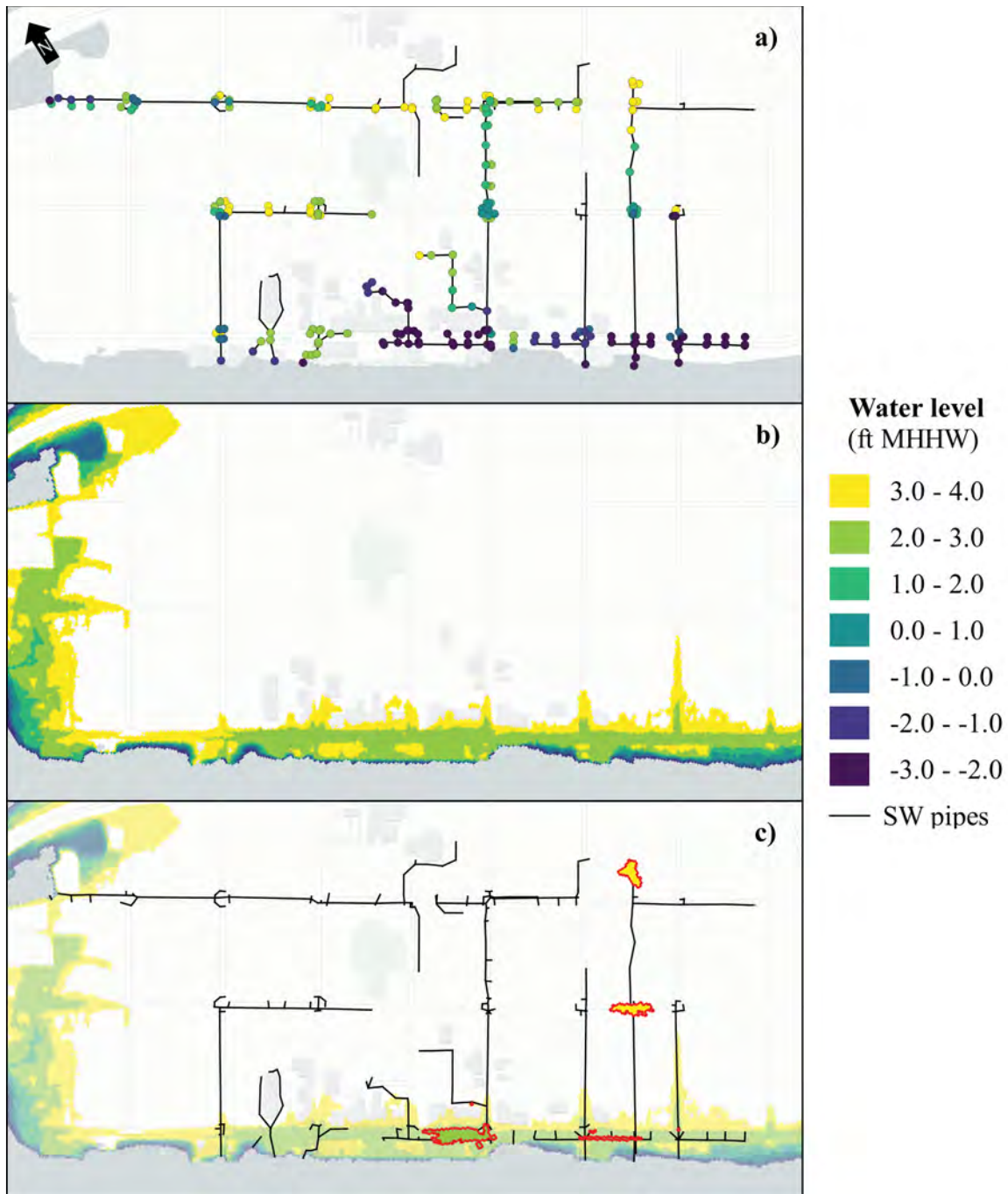
323



324

325 **Figure 4.** Model results for Beaufort, NC. Estimated impact of water level on stormwater inlets  
 326 in Beaufort, NC across a range of water levels modeled with (stacked bars) and without (black  
 327 dots/line) incorporating the stormwater network. NOAA HTF threshold for Beaufort is shown as  
 328 black vertical bar (1.77 ft). Yellow bars (“100+” volume filled) indicate full/surcharging inlets.  
 329





330

331 **Figure 5.** Spatial model results from Beaufort, NC. **a)** Water level of first impact (any degree of  
 332 inundation) for pipe ends, **b)** overland flooding ignoring the stormwater network connected to  
 333 Taylor's Creek for each water level, and **c)** extent of ponding at each water level due to  
 334 surcharge from stormwater network (red border) and overland flooding (transparent).  
 335

336

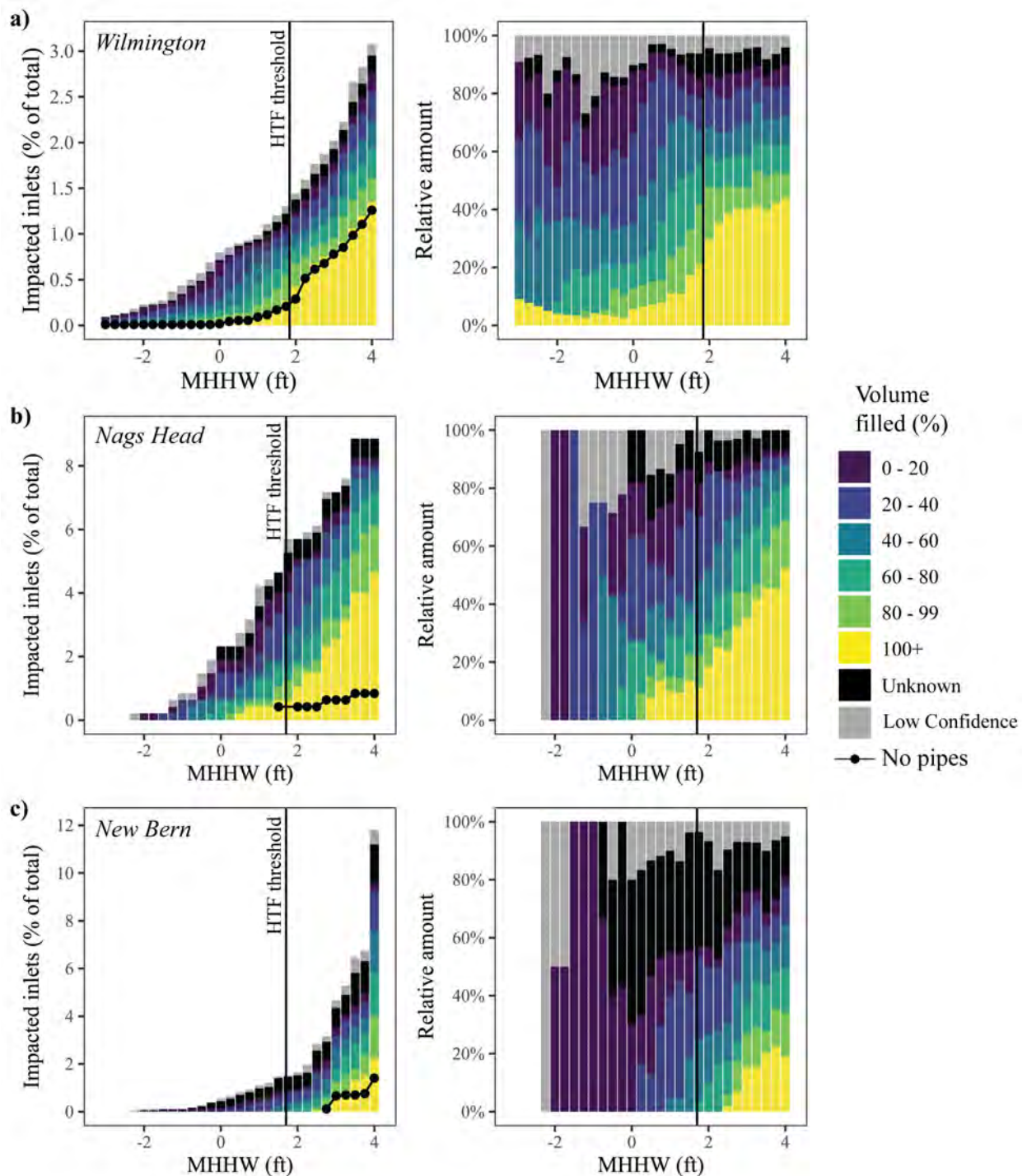
Inundation modeling in Wilmington, New Bern, and Nags Head showed that stormwater

337

network inundation likely also occurs often in these cities at typical water levels, but the percent

338 of infrastructure impacted is lower than in Beaufort (Figure 6 – note the different vertical scales  
339 for each municipality). As in Beaufort, all of the study cities had extensive estimated subsurface  
340 inundation at typical water levels, and most estimated inundation did not result in overland  
341 flooding (Figure 6). Comparing model simulations that incorporate the stormwater network with  
342 model simulations that do not showed that estimates of stormwater inlet surcharge in  
343 Wilmington and New Bern aligned well. Similar to Beaufort, though, the estimated number of  
344 surcharging/full structures in Nags Head as estimated by model simulations that incorporate the  
345 stormwater network was much higher than predicted by flooding estimates that do not  
346 incorporate the stormwater network (Figure 6).

347



348

349 **Figure 6.** Model results from Wilmington, Nags Head, and New Bern, NC. Estimated impact of  
 350 water level on stormwater inlets across a range of water levels in **a)** Wilmington, **b)** Nags Head,  
 351 and **c)** New Bern, NC. Impacts were modeled with (stacked bars) and without (black dots/line)  
 352 incorporating the stormwater network. NOAA HTF threshold (1.84 ft – Wilmington) and

353 approximate HTF threshold (1.7 ft – Nags Head and New Bern) shown as black vertical bar.  
354 Yellow bars (“100+” volume filled) indicate full/surcharging inlets.  
355

#### 356 **4 Discussion**

357 Inundation of stormwater infrastructure can have a large local impact on the frequency  
358 and magnitude of urban flooding, but this phenomenon remains difficult to characterize. Using  
359 national high tide flooding and road data, this study demonstrated that tidal inundation on coastal  
360 roads, and thus stormwater infrastructure, occurs in municipalities along the east coast of the US.  
361 Measuring stormwater infrastructure inundation at a local scale in Beaufort, NC, gauged  
362 stormwater outfalls were inundated by the tide daily while the monitored upstream storm drain  
363 was inundated during extreme high tides. Predictions of pipe water level based on local NOAA  
364 water level data and pipe elevations showed that predicted outfall water levels corresponded well  
365 with measured water levels, but predicted water levels for the upstream storm drain were slightly  
366 higher than measured water levels, highlighting an acknowledged weakness of static inundation  
367 models. Using a 2D static inundation model coupled with a 1D stormwater network model (see  
368 Methods), we found that all four study municipalities likely experience frequent inundation of  
369 underground stormwater infrastructure that impairs their ability to convey stormwater.  
370 Inundation of the underground stormwater network occurred at water levels far below local  
371 NOAA “minor flooding” thresholds (~ 1.75 ft above MHHW), suggesting that current and future  
372 estimates of high tide flooding extent and frequency may drastically underestimate urban flood  
373 risk due to reduced stormwater capacity. While stormwater networks aim to drain stormwater  
374 runoff, model results from Beaufort and Nags Head showed that the stormwater network can act  
375 as a conduit for elevated downstream waters to flood low-lying inland areas that would otherwise  
376 be disconnected from receiving waters. Overall, this study shows that stormwater network

377 inundation in coastal US municipalities is common and can increase the risk of overland  
378 flooding.

379

#### 380 4.1. Impacts of network inundation

381 The measured and estimated stormwater network inundation in this study demonstrate the  
382 frequency of stormwater network inundation and the associated decrease in network drainage  
383 during wet weather along the east coast of the US. It is well-known that elevated water levels are  
384 a major driver of coastal urban flooding during extreme storm events such as hurricanes (Shen et  
385 al., 2019), but this study further shows that stormwater networks may often have reduced  
386 capacity to convey runoff during typical weather conditions and water levels far below local  
387 NOAA “minor flooding” thresholds frequently used to characterize high tide flooding (e.g.,  
388 Sweet et al., 2018). Storm surge is not required to impair stormwater network drainage; typical  
389 high tides can affect network drainage during wet weather even absent overland flooding due to  
390 tides. Although Beaufort had the largest estimated impact at typical water levels (< 1 ft MHHW),  
391 it is important to note that it was the smallest of the four study municipalities with most of the  
392 surveyed infrastructure in the downtown portion of the municipality along a developed  
393 waterfront. A low percent of impacted stormwater inlets in another municipality could still mean  
394 a large impact in specific lower-lying spots within the municipality, especially if the municipality  
395 also encompasses inland area with higher elevations (e.g., Wilmington).

396 Inundation estimates of infrastructure in the study cities, especially Beaufort and Nags  
397 Head, also suggest that the stormwater network may act as conduit for receiving waters to flood  
398 low-lying areas at high water levels. Both of these municipalities had approximately 1% of their  
399 total road area impacted by HTF, suggesting that this specific issue may be widespread given  
400 that 1/3<sup>rd</sup> of the incorporated municipalities along the US east coast that experience HTF on

401 roads had similar or greater levels of HTF impact on total road area. This overland flooding that  
402 is counterintuitively exacerbated by stormwater networks could have negative impacts during  
403 both dry and wet weather. During dry weather, this overland “nuisance” flooding could have  
404 negative economic impacts for local businesses by limiting access (Hino et al., 2019). During  
405 wet weather, this overland flooding would effectively reduce the ability of the surrounding area  
406 to drain, depending on the amount of precipitation. An example of this high-tide flooding via the  
407 stormwater network is evident in Beaufort, where a section of road adjacent to Taylor’s Creek  
408 (Front St.) is predicted to flood at 1-2 ft MHHW (Figure 5b). These model results align with high  
409 tide flood reports at this location (Figure S3) and NOAA estimates of high tide flooding during  
410 dry weather (<https://bit.ly/30MWUGi>).

411         During dry weather, the inundation of subsurface pipes with brackish or saltwater at  
412 typical tidal water levels can degrade them (Bjerklie et al., 2012) and promote saltwater intrusion  
413 and the transmission of fecal bacteria from nearby sewer lines (Su et al., 2020). We did not  
414 directly measure or model either of these effects, but during water level data collection in  
415 Beaufort, we did find qualitative evidence of network degradation in the form of oysters and  
416 barnacles growing within the stormwater network or cracked pipes (Figures S4-S6). The issue of  
417 stormwater and sanitary sewer degradation from inundation likely exists in Beaufort, as a  
418 previous study in the area measured high levels of human-sourced fecal indicator bacteria in  
419 piped stormwater runoff (Parker et al., 2010).

420

#### 421         4.2 Issues characterizing network inundation

422         While inundation of stormwater networks appears widespread and common in our study  
423 area, directly characterizing the scale of the issue of stormwater network inundation remains a  
424 challenge due to issues of data quality and availability.

425           Good quality stormwater network data is key to assessing the impacts of inundation on  
426 the stormwater network, but inadequate funding likely hinders the collection of stormwater  
427 infrastructure survey measurements. For example, in NC, many municipalities raise the majority  
428 of funding for stormwater management directly through local stormwater fees (Riggs & Kirk,  
429 2019). While stormwater fees are a common means of raising funding for stormwater projects,  
430 they often do not generate enough funding for necessary stormwater infrastructure projects  
431 (Riggs & Kirk, 2019; Zhao et al., 2019). Approximately 18% of stormwater fees tracked over the  
432 past decade in NC have not been increased during that time period, and 36% of the fees that have  
433 been increased did not keep pace with inflation despite rising budget needs (Riggs & Kirk,  
434 2019). Also, municipality size and property values likely both contribute to higher stormwater  
435 fees (Kea et al., 2016), thus allowing more populous cities or areas with higher property values  
436 to collect more money for stormwater projects than smaller towns with lower property values,  
437 despite the fact that smaller towns are more likely to have a higher degree of road impacts from  
438 HTF (Figure 2c).

439           If municipalities do, in fact, have adequate stormwater network data to assess the possible  
440 impacts of inundation, there are currently no centralized state or federal databases to house the  
441 data. A public database of stormwater network data would have a positive impact on planning  
442 efforts to increase resilience to extreme storm events and sea level rise by allowing comparisons  
443 of network inundation between municipalities and additional modeling of flood risks.  
444 Comparisons of network inundation risk could help determine which municipalities are most at  
445 risk and in need of additional funding for updates. Broad access to stormwater network datasets  
446 would also allow more researchers access to undertake more sophisticated modelling of real-  
447 world flooding conditions during storm events (e.g., Shen et al., 2019). Stormwater networks are

448 heterogeneous due to differences in development or landscape properties, so infrastructure data  
449 from more municipalities could improve the accuracy of large-scale estimates that rely on  
450 assumptions of stormwater network characteristics. For the current study, we assume that HTF  
451 on municipal roads is an indicator of stormwater network inundation that drains the surrounding  
452 area, and additional infrastructure data from more municipalities would allow this assumption to  
453 be tested more broadly.

454

#### 455 4.3 Addressing network inundation in the short- and long-term

456 The threat of coastal flooding is increasing due to rising seas and the effects of climate  
457 change on precipitation patterns (Kulp & Strauss, 2019; Nicholls et al., 1999; Sweet et al., 2020,  
458 2018; Wahl et al., 2015; Woodruff et al., 2013), and many low-lying coastal areas will need to  
459 adapt quickly to both increased stormwater network inundation and excessive stormwater runoff.

460 For stormwater network inundation in the short term, the most direct engineering solution  
461 is to install tide gates that prevent flow up-network when receiving water levels are elevated.  
462 These tide gates reduce tidal inundation (Sadler et al., 2020; Shen et al., 2019), and there are  
463 even efforts to make these tide gates responsive to current and predicted inundation to increase  
464 their efficacy (Sadler et al., 2020). Though this retrofit to the current stormwater network may be  
465 effective in the short- to medium-term, predicted increases in sea level and groundwater will  
466 inevitably lead to continuously inundated outfalls in vulnerable locations and decreased surface  
467 storage of stormwater further inland (Davtalab et al., 2020; Rotzoll & Fletcher, 2013).

468 Addressing the long-term issue of coastal urban flooding, which includes both  
469 stormwater network inundation and excess stormwater runoff volumes, will require substantial  
470 investment in planning and upgrading drainage systems (Robert L Wilby & Keenan, 2012). A  
471 discussion of this broader adaptation and planning effort is outside the scope of the current study,



472 but these strategies broadly include updating infrastructure to address network inundation (e.g.,  
473 backflow prevention, pumping), decentralized or low impact development to manage stormwater  
474 (e.g., stormwater harvesting), landscape-scale planning to incorporate surface storage of flood  
475 waters, and possibly managed retreat or buyouts of vulnerable areas (Rogers et al., 2020;  
476 Rosenzweig et al., 2018; Robert L Wilby & Keenan, 2012).

477 Future investigation is needed to further characterize the extent of coastal stormwater  
478 network inundation to inform planning efforts, and the simple modeling framework presented  
479 here can be used as an initial step for both municipalities and researchers.

480

#### 481 **Acknowledgments, Samples, and Data**

482 We thank Drs. Miyuki Hino and Katherine Anarde for offering comments on previous  
483 versions of the manuscript. This research was supported by NOAA NERRS Science  
484 Collaborative and the North Carolina Policy Collaboratory. All data, code, and materials used in  
485 the analyses will be available on GitHub and Zenodo.org prior to publication.

486

487

#### 488 **References**

489

- 490 Bjerklie, D. M., Mullaney, J. R., Stone, J. R., Skinner, B. J., & Ramlow, M. A. (2012).  
491 *Preliminary Investigation of the Effects of Sea-Level Rise on Groundwater Levels in New*  
492 *Haven, Connecticut.*
- 493 Burns, M. J., Fletcher, T. D., Walsh, C. J., Ladson, A. R., & Hatt, B. E. (2012). Hydrologic  
494 shortcomings of conventional urban stormwater management and opportunities for reform.  
495 *Landscape and Urban Planning, 105*(3), 230–240.  
496 <https://doi.org/10.1016/j.landurbplan.2011.12.012>
- 497 Castrucci, L., & Tahvildari, N. (2018). Modeling the impacts of sea level rise on storm surge  
498 inundation in flood-prone urban areas of Hampton roads, Virginia. *Marine Technology*  
499 *Society Journal, 52*(2), 92–105. <https://doi.org/10.4031/MTSJ.52.2.11>
- 500 Davtalab, R., Mirchi, A., Harris, R. J., Troilo, M. X., & Madani, K. (2020). Sea Level Rise  
501 Effect on Groundwater Rise and Stormwater Retention Pond Reliability. *Water, 12*(4),

- 502 1129. <https://doi.org/10.3390/w12041129>
- 503 Eggleston, J., & Pope, J. (2013). *Land Subsidence and Relative Sea-Level Rise in the Southern*  
504 *Chesapeake Bay Region. USGS Circular 1392.*
- 505 Gallien, T. W., Sanders, B. F., & Flick, R. E. (2014). Urban coastal flood prediction: Integrating  
506 wave overtopping, flood defenses and drainage. *Coastal Engineering, 91*, 18–28.  
507 <https://doi.org/10.1016/j.coastaleng.2014.04.007>
- 508 Hale, R. L. (2016). Spatial and temporal variation in local stormwater infrastructure use and  
509 stormwater management paradigms over the 20th century. *Water (Switzerland), 8*(7).  
510 <https://doi.org/10.3390/w8070310>
- 511 Hallegatte, S., Green, C., Nicholls, R. J., & Corfee-Morlot, J. (2013). Future flood losses in  
512 major coastal cities. *Nature Climate Change, 3*(9), 802–806.  
513 <https://doi.org/10.1038/nclimate1979>
- 514 Hasan Tanim, A., & Goharian, E. (2020). Developing a hybrid modeling and multivariate  
515 analysis framework for storm surge and runoff interactions in urban coastal flooding.  
516 *Journal of Hydrology*, (October), 125670. <https://doi.org/10.1016/j.jhydrol.2020.125670>
- 517 Hinkel, J., Lincke, D., Vafeidis, A. T., Perrette, M., Nicholls, R. J., Tol, R. S. J., ... Levermann,  
518 A. (2014). Coastal flood damage and adaptation costs under 21st century sea-level rise.  
519 *Proceedings of the National Academy of Sciences of the United States of America, 111*(9),  
520 3292–3297. <https://doi.org/10.1073/pnas.1222469111>
- 521 Hino, M., Belanger, S. T., Field, C. B., Davies, A. R., & Mach, K. J. (2019). High-tide flooding  
522 disrupts local economic activity. *Science Advances, 5*(2), 1–10.  
523 <https://doi.org/10.1126/sciadv.aau2736>
- 524 Jacobs, J. M., Cattaneo, L. R., Sweet, W., & Mansfield, T. (2018). Recent and future outlooks for  
525 nuisance flooding impacts on roadways on the U.S. east coast. *Transportation Research*  
526 *Record, 2672*(2), 1–10. <https://doi.org/10.1177/0361198118756366>
- 527 Kea, K., Dymond, R., & Campbell, W. (2016). An Analysis of Patterns and Trends in United  
528 States Stormwater Utility Systems. *Journal of the American Water Resources Association,*  
529 *52*(6), 1433–1449. <https://doi.org/10.1111/1752-1688.12462>
- 530 Kulp, S. A., & Strauss, B. H. (2019). New elevation data triple estimates of global vulnerability  
531 to sea-level rise and coastal flooding. *Nature Communications, 10*(1).  
532 <https://doi.org/10.1038/s41467-019-12808-z>
- 533 Milly, P. C. D., Betancourt, J., Falkenmark, M., Hirsch, R. M., Kundzewicz, Z. W., Lettenmaier,  
534 D. P., & Stouffer, R. J. (2008). Climate change: Stationarity is dead: Whither water  
535 management? *Science, 319*(5863), 573–574. <https://doi.org/10.1126/science.1151915>
- 536 Nicholls, R. J., Hoozemans, F. M. J., & Marchand, M. (1999). Increasing flood risk and wetland  
537 losses due to global sea-level rise: Regional and global analyses. *Global Environmental*

- 538 *Change*, 9(SUPPL.). [https://doi.org/10.1016/S0959-3780\(99\)00019-9](https://doi.org/10.1016/S0959-3780(99)00019-9)
- 539 Parker, J. K., McIntyre, D., & Noble, R. T. (2010). Characterizing fecal contamination in  
540 stormwater runoff in coastal North Carolina, USA. *Water Research*, 44(14), 4186–4194.  
541 <https://doi.org/10.1016/j.watres.2010.05.018>
- 542 Pebesma, E. (2018). Simple Features for R: Standardized Support for Spatial Vector Data. *The R*  
543 *Journal*, 10(1), 439. <https://doi.org/10.32614/RJ-2018-009>
- 544 Riggs, E., & Kirk, E. (2019). *The Stormwater Finance Landscape : Where we've come from and*  
545 *where we've yet to go*. Chapel Hill.
- 546 Rogers, B. C., Bertram, N., Gersonius, B., Gunn, A., Löwe, R., Murphy, C., ... Arnbjerg-  
547 Nielsen, K. (2020). An interdisciplinary and catchment approach to enhancing urban flood  
548 resilience: A Melbourne case. *Philosophical Transactions of the Royal Society A:*  
549 *Mathematical, Physical and Engineering Sciences*, 378(2168).  
550 <https://doi.org/10.1098/rsta.2019.0201>
- 551 Rosenzweig, B. R., McPhillips, L., Chang, H., Cheng, C., Welty, C., Matsler, M., ... Davidson,  
552 C. I. (2018). Pluvial flood risk and opportunities for resilience. *Wiley Interdisciplinary*  
553 *Reviews: Water*, (June), e1302. <https://doi.org/10.1002/wat2.1302>
- 554 Rotzoll, K., & Fletcher, C. H. (2013). Assessment of groundwater inundation as a consequence  
555 of sea-level rise. *Nature Climate Change*, 3(5), 477–481.  
556 <https://doi.org/10.1038/nclimate1725>
- 557 Sadler, J. M., Goodall, J. L., Behl, M., Bowes, B. D., & Morsy, M. M. (2020). Exploring real-  
558 time control of stormwater systems for mitigating flood risk due to sea level rise. *Journal of*  
559 *Hydrology*, 583(January). <https://doi.org/10.1016/j.jhydrol.2020.124571>
- 560 Schmid, K., Hadley, B., & Waters, K. (2014). Mapping and portraying inundation uncertainty of  
561 bathtub-type models. *Journal of Coastal Research*, 30(3), 548–561.  
562 <https://doi.org/10.2112/JCOASTRES-D-13-00118.1>
- 563 Shen, Y., Morsy, M. M., Huxley, C., Tahvildari, N., & Goodall, J. L. (2019). Flood risk  
564 assessment and increased resilience for coastal urban watersheds under the combined  
565 impact of storm tide and heavy rainfall. *Journal of Hydrology*, 579(June), 124159.  
566 <https://doi.org/10.1016/j.jhydrol.2019.124159>
- 567 Su, X., Liu, T., Beheshti, M., & Prigiobbe, V. (2020). Relationship between infiltration, sewer  
568 rehabilitation, and groundwater flooding in coastal urban areas. *Environmental Science and*  
569 *Pollution Research*, 27(13), 14288–14298. <https://doi.org/10.1007/s11356-019-06513-z>
- 570 Sweet, W., Dusek, G., Carbin, G., Marra, J., Marcy, D., & Simon, S. (2020). *2019 State of U.S.*  
571 *High Tide Flooding with a 2020 Outlook* (Vol. NOAA Techn).
- 572 Sweet, W. V., Dusek, G., Obeysekera, J., & Marra, J. J. (2018). *Patterns and projections of high*  
573 *tide flooding along the U.S. coastline using a common impact threshold*.

- 574 Titus, J. G., Kuo, C. Y., Gibbs, M. J., LaRoche, T. B., Webb, M. K., & Waddell, J. O. (1987).  
575 Greenhouse effect, sea level rise, and coastal drainage systems. *Journal of Water Resources*  
576 *Planning and Management*, 113(2), 216–227. [https://doi.org/10.1061/\(ASCE\)0733-](https://doi.org/10.1061/(ASCE)0733-9496(1987)113:2(216))  
577 9496(1987)113:2(216)
- 578 Wahl, T., Jain, S., Bender, J., Meyers, S. D., & Luther, M. E. (2015). Increasing risk of  
579 compound flooding from storm surge and rainfall for major US cities. *Nature Climate*  
580 *Change*, 5(12), 1093–1097. <https://doi.org/10.1038/nclimate2736>
- 581 Wdowinski, S., Bray, R., Kirtman, B. P., & Wu, Z. (2016). Increasing flooding hazard in coastal  
582 communities due to rising sea level: Case study of Miami Beach, Florida. *Ocean and*  
583 *Coastal Management*, 126(June), 1–8. <https://doi.org/10.1016/j.ocecoaman.2016.03.002>
- 584 Wilby, R.L. (2007). A Review of Climate Change Impacts on the Built Environment. *Built*  
585 *Environment*, 33(1), 31–45. <https://doi.org/10.2148/benv.33.1.31>
- 586 Wilby, Robert L, & Keenan, R. (2012). Adapting to flood risk under climate change. *Progress in*  
587 *Physical Geography*. <https://doi.org/10.1177/0309133312438908>
- 588 Woodruff, J. D., Irish, J. L., & Camargo, S. J. (2013). Coastal flooding by tropical cyclones and  
589 sea-level rise. *Nature*, 504(7478), 44–52. <https://doi.org/10.1038/nature12855>
- 590 Zervas, C. (2009). Sea Level Variations of the United States 1854-2006. *Technical Report NOS*  
591 *CO-OPS 053*, 53(December).
- 592 Zhao, J. Z., Fonseca, C., & Zeerak, R. (2019). Stormwater utility fees and credits: A funding  
593 strategy for Sustainability. *Sustainability (Switzerland)*, 11(7).  
594 <https://doi.org/10.3390/su11071913>

595